International Journal of Manufacturing Economics and Management
ISSN 2784-1278 ISSN-L 2784-1278, Vol. IV, No. 2 / 2024
https://doi.org/10.54684/ijmem.2024.4.2.88

ON THE ABILITY OF DIFFERENTIAL TRANSFORM METHOD AND ITS IMPROVEMENTS TO SOLVE PROPERLY THE SHIP'S ROLL EQUATION

Dumitru Deleanu, Constantin Louis Dumitrache, Mihaela Turof

Constanta Maritime University, Department of General Engineering Sciences, Mircea cel Batran street, No. 104, 900663, Romania

Corresponding author: Dumitru Deleanu, dumitrudeleanu@yahoo.com

Abstract: A major concern regarding the ship safety is related to severe rolling oscillations which, in certain circumstances, can even lead to its capsizing. Assuming the rolling motion decoupled from its other five possible motions, one results a mathematical model associated to a second order differential equation where the main parameters (inertia, damping, stiffness and excitation) reveal a significant nonlinearity. In the absence of exact analytical solutions, the amplitude and period characteristics of the ship rolling can be evaluated by approximate numerical or analytical methods. In this work, we checked if the performant differential transform method (DTM) and its improvement with Pade approximants is able to provide approximate analytical solutions for nonlinear roll equation, valid for both the transitory and stationary states. The obtained results were verified against those produced by MatLab numerical generated simulations. We noticed that for the linearized roll equation, which describes quite correctly a significant part of the situations of practical interest, the DTM doubled by the Pade approximation [4/4] offers the exact solution. If the nonlinear terms from damping and restoring moments are included in the study but the sea is considered waveless, the investigated technique proves a good accuracy in describing the attenuation over time of the initial excitation. DTM and Pade [4/4] cease to offer reasonable solutions as soon as the exciting moment of the waves is included in the procedure. We gave clear explanations for this impasse and showed that the use of higher-order Pade approximations can solve (even if with additional efforts) totally or at least partially this problem.
Key words: ship rolling, approximate solution, differential transform method.

1. INTRODUCTION

The roll motion of a vessel in beam regular waters can be represented quite accurately by a second-order non-linear differential equation with the roll angle as independent variable and nonlinear terms determined by the models used for damping and restoring moments. Such kind of equation has been solved in the literature both by numerically and analytically techniques, each havind disavantages and limitations [1 – 6].

In the present work, we concentrated on a semi-analytical approach proposed by Zhou [7] for initial value problems in electrical engineering, called *differential transform method* (DTM for short). This technique gives the solution as a power series around an arbitrary point in the variable domain (usually the origin). Inevitably, the founded solution diverges relatively quickly by using the first few components of the series so that modifications were thought by researchers to grow the radius of convergence. A remarkable improvement was suggested by El-Shahed [8], who put together DTM with Laplace transform and Pade approximants to closely estimate the solution of a differential equation by a small number of terms without using classical ideas as liniarization, discretization, perturbation, round – off errors and so on. Another improvement is due to Gokdogan et al. [9] and consists in dividing the domain of variables into small domains so the center of the series changes on each subdomain and the independent variables remain relatively close to the center. The drawback of this technique is the large number of subintervals required for accurate results. To overcome it, Khatami et al. [10] used trigonometric functions instead of polynomial ones and succedded to significantly increase the quality of the solution.

The rest of the paper is organized as follows: In the next section the basic ideas of DTM and Pade approximants are briefly described. In Section 3, the DTM and its improvements are implemented to solve the roll equation in different scenarios. The obtain results are put face to face with the numerical ones provided by the ode 45 solver in Matlab. Finally, the Section 4 brings together the main conclusions of the study.

2. MATERIALS AND METHODS

2.1 Basic idea of the differential transform method

An infinitely continuously differentiable function $u: D \rightarrow R$ can be developed in a Taylor series with the center in point $x_0 \in D$ of form:

$$u(x) = \sum_{k=0}^{\infty} \frac{1}{k!} \frac{d^k u(x)}{dx^k}\Bigg|_{x=x_0} \cdot (x - x_0)^k \tag{1}$$

The differential transform of *u(x)* is defined as by:

$$U(k) = \frac{1}{k!} \frac{d^k u(x)}{dx^k}\Bigg|_{x=x_0}, k \in N \tag{2}$$

u(x) is called the original function while *U(k)* is the transformed function. The differential inverse transform of *U(k)* is given by

$$u(x) = \sum_{k=0}^{\infty} U(k)(x - x_0)^k \tag{3}$$

Typically, the value $x_0 = 0$ is chosen. In concrete problems, the function *u(x)* is expressed by a finite series

$$u(x) \cong \sum_{k=0}^{m} U(k)(x - x_0)^k \tag{4}$$

The number of terms *m* is determined by the rate of convergence of the series. When apply the DTM to a differential equation, this is converted into an algebraic equation in the variable *k* and unknown *U(k)*. The latter will be obtained recursively.

The most used operations performed by DTM and which are also necessary in the present study are listed below:

(i) If $w(x) = u(x) \pm v(x)$, then $W(k) = U(k) \pm V(k)$;

(ii) If $w(x) = \lambda\, u(x)$, then $W(k) = \lambda\, U(k), \lambda$ constant;

(iii) If $w(x) = \dfrac{d^n u(x)}{dx^n}$, then $W(k) = (k+1)(k+2) \cdot \ldots \cdot (k+n) U(k+n)$;

(iv) If $w(x) = \cos(\omega\, x + \varphi)$, then $W(k) = \dfrac{\omega^k}{k!} \cos\left(\dfrac{\pi\, k}{2} + \varphi\right)$, ω, φ constants.

2.2 Pade's approximants

Let *f* be a function represented as a power series, $f(x) = \sum_{i=0}^{\infty} a_i\, x^i$. A Pade approximant [L, M] associated to *f* is a rational function of the form $[L, M] = \dfrac{P_L(x)}{Q_M(x)}$, where P_L and Q_M are polynomials of degree at most *L*, respectively *M*. More precisely:

$$P_L(x) = p_0 + p_1 x + p_2 x^2 + \ldots + p_L x^L, Q_M(x) = q_0 + q_1 x + q_2 x^2 + \ldots + q_M x^M \tag{5}$$

By amplifying the fraction P_L / Q_M with a suitable constant, $q_0 = 1$ can be obtained, which would reduce the number of unknown coefficients in P_L and Q_M to *L* + *M* +1. From the formal equality

$$f(x) = P_L(x)/Q_M(x) \Leftrightarrow (a_0 + a_1 x + a_2 x^2 + \ldots)(1 + q_1 x + \ldots + q_M x^M) = p_0 + p_1 x + \ldots + p_L x^L + O(x^{L+M+1})$$

by equating the coefficients of terms having the same degree, one obtains the system

$$\begin{cases} a_0 = p_0 \\ a_1 + a_0 q_1 = p_1 \\ a_2 + a_1 q_1 + a_0 q_2 = p_2 \\ \dots\dots\dots \\ a_L + a_{L-1} q_1 + \dots + a_0 q_L = p_L \end{cases} \quad \text{and} \quad \begin{cases} a_{L+1} + a_L q_1 + \dots + a_{L-M+1} q_M = 0 \\ a_{L+2} + a_{L+1} q_1 + \dots + a_{L-M+2} q_M = 0 \\ \dots\dots\dots \\ a_{L+M} + a_{L+M-1} q_1 + \dots + a_L q_M = 0 \end{cases} \tag{6}$$

in $q_i, i = \overline{1,M}$ and $p_j, j = \overline{1,L}$.

It is obvious that different choices for L and M will lead to different approximants. To the question "*What is the best selection for L and M?*" a partial answer is "*L* = *M*". In addition, the numerical results presented in the specialized literature show that the higher the values of *L* and *M* are, the better approximations are obtained for the exact solution of the differential equation.

2.3 The ship's roll equation

The ship rolling in a regular wave can be described precisely enough by the second order differential equation:

$$\ddot{\theta} + d_1 \dot{\theta} + d_3 \dot{\theta}^3 + k_1 \theta + k_3 \theta^3 = m \cos \omega t, \ \theta(0) = \theta_0, \dot{\theta}(0) = \dot{\theta}_0 \tag{7}$$

where d_1 and d_3 denote the linear and cubic roll damping coefficients, k_1 and k_3 the roll restoring moment coefficients, *m* and ω the forcing amplitude and wave frequency, respectively. In addition, θ is the roll angle and an overdot signifies the time differentiation.

For numerical simulations, the coefficients $d_i, i = 1,3$ and $k_i, i = 1,3$ were adopted for a real ferry ship [11, 12]:

$$d_1 = 0.01265913 \ s^{-1}, \ d_3 = 0.4954 \ s, k_1 = 0.691997033 \ s^{-2}, k_3 = -0.53920393 \ s^{-2}$$

3. RESULTS AND DISCUSSION

Applying the DTM to roll equation (7) yields the following recursive scheme:

$$(k+2)(k+1)\theta(k+2) + d_1 (k+1)\theta(k+1) + d_3 \sum_{s=0}^{k} \sum_{i=0}^{s} (i+s)(s-i+1)(k-s+1)\theta(i+1)\theta(s-i+1)\theta(k-s+1) +$$

$$+ k_1 \theta(k) + k_3 \sum_{s=0}^{k} \sum_{i=0}^{s} \theta(i)\theta(s-i)\theta(k-s) = m \frac{\omega^k}{k!} \cos\left(\frac{\pi k}{2}\right) \tag{8}$$

$$\theta(0) = \theta_0, \theta(1) = \dot{\theta}_0 \tag{9}$$

Considering $k = 0,1,\dots,5$ one finds the next terms involved in the series (4):

$$\begin{aligned}
&k = 0: 2\theta(2) + d_1 \theta(1) + d_3 \theta^3(1) + k_1 \theta(0) + k_3 \theta^3(0) = m \\
&k = 1: 6\theta(3) + 2d_1 \theta(2) + 6d_3 \theta^2(1)\theta(2) + k_1 \theta(1) + 3k_3 \theta^2(0)\theta(1) = 0 \\
&k = 2: 12\theta(4) + 3d_1 \theta(3) + 3d_3 \left(3\theta^2(1)\theta(3) + 4\theta(1)\theta^2(2)\right) + k_1 \theta(2) + 3k_3 \left(\theta^2(0)\theta(2) + \theta(0)\theta^2(1)\right) = -\frac{a\omega^2}{2} \\
&k = 3: 20\theta(5) + 4d_1 \theta(4) + d_3 \left(12\theta^2(1)\theta(4) + 8\theta^3(2) + 36\theta(1)\theta(2)\theta(3)\right) + k_1 \theta(3) + \\
&\qquad + k_3 \left(3\theta^2(0)\theta(3) + \theta^3(1) + 6\theta(0)\theta(1)\theta(2)\right) = 0 \\
&k = 4: 30\theta(6) + 5d_1 \theta(5) + d_3 \left(15\theta^2(1)\theta(5) + 48\theta(1)\theta(2)\theta(4) + 27\theta(1)\theta^2(3) + 36\theta^2(2)\theta(3)\right) + k_1 \theta(4) + \\
&\qquad + k_3 \left(3\theta^2(0)\theta(4) + 6\theta(0)\theta(1)\theta(3) + 3\theta(0)\theta^2(2) + 3\theta^2(1)\theta(2)\right) = m\frac{\omega^4}{24} \\
&k = 5: 42\theta(7) + 6d_1 \theta(6) + d_3 \left(18\theta^2(1)\theta(6) + 60\theta(1)\theta(2)\theta(5) + 72\theta(1)\theta(3)\theta(4) + 48\theta^2(2)\theta(4) + \right. \\
&\left. + 54\theta(2)\theta^2(3)\right) + k_1 \theta(5) + k_3 \left(3\theta^2(0)\theta(5) + 6\theta(0)\theta(1)\theta(4) + 6\theta(0)\theta(2)\theta(3) + 3\theta^2(1)\theta(3) + 3\theta(1)\theta^2(2)\right) = 0
\end{aligned} \tag{10}$$

In what follows, we will exemplify the algorithm of DTM in three situations. In the first, we will approach the linear roll equation that is, we will impose that $d_3 = k_3 = 0$. In the second, we will include the nonlinear terms in the study, but we will omit the perturbing moment of waves (m = 0). The solution given by DTM and its improvements to the full roll equation will represent the last analysed case.

Case I: $d_3 = k_3 = 0$
Equation (7) reduces to:

$$\ddot{\theta} + d_1 \dot{\theta} + k_1 \theta = m \cos \omega t, \theta(0) = \theta_0, \dot{\theta}(0) = \dot{\theta}_0 \tag{11}$$

and has the exact solution:

$$\theta_{exact}(t) = a \exp\left(-\frac{d_1}{2} t\right) \sin(\omega_d t + \varphi) + A \sin(\omega t + \phi) \tag{12}$$

with

$$\omega_d = \sqrt{k_1 - d_1^2 / 4}, \ A = \frac{m}{\sqrt{(k_1 - \omega^2)^2 + (d_1 \omega)^2}}, \phi = a \tan \frac{d_1 \omega}{k_1 - \omega^2}$$

and a, respectively φ, constants provided by initial conditions.
The linear equation (11) represents a good substitution for (7) if the oscillation amplitudes do not exceed 10^0 – 15^0, which covers a significant part of the situations encountered on sea.
Figure 1, which shows the roll amplitudes for the two models and for a wide range of pairs (ω, m) reinforces the previous statement. Notable differences between the two panels appear only in the area of amplitudes over 30^0, which rather represent the exception (see also Table 1). The grid used in Figure 1 contains 201 x 201 = 40401 combinations (ω, m).

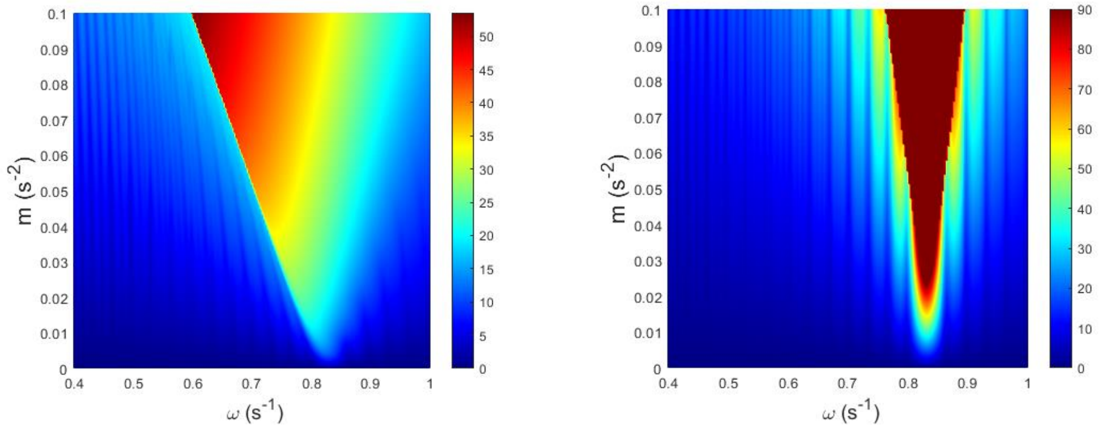

(a) (b)

Fig. 1. The roll amplitudes determined with the nonlinear model (a), respective linear one (b), for $\omega \in [0.4, 1.0]$ and $0 \le m \le 0.1$

Subcase 1.1: $\omega = 0.4, m = 0.05, \theta(0) = 0.1, \dot{\theta}(0) = 0$
For this pair (ω, m), $\theta(t)$ given by DTM is

$$\theta_{DTM}(t) = 0.1 - 0.0096 t^2 + 0.4051 \cdot 10^{-3} t^3 + 0.2201 \cdot 10^{-3} t^4 - 0.1959 \cdot 10^{-5} t^5 - 0.3296 \cdot 10^{-5} t^6 + \\ + 0.382 \cdot 10^{-7} t^7 + 0.356 \cdot 10^{-7} t^8 \tag{13}$$

Figure 2*a* shows a comparison between the results provided by *ode45 solver* in Matlab and DTM approach. The two solutions are close enough only for t < 5 after which, due to the high power of time variable, the DTM solution diverges.

Table 1. The distribution of roll amplitudes in value groups. The presented values were obtained from 40401 combinations (ω, m)

Amplitude	0^0 - 15^0	15^0 - 30^0	30^0 - 50^0	50^0 - 90^0	> 90^0
Nonlinear model	24504 (60.05%)	8827 (21.85%)	6825 (16.89%)	245 (0.61%)	0 (0%)
Linear model	25291 (62.60%)	9224 (22.83%)	3657 (9.05%)	1169 (2.89%)	1060 (2.62%)

The last one can be improved with the help of Pade approximants. If Pade [3/3] is selected, then:

$$\left[\frac{3}{3}\right] = \frac{0.1s^2 + 0.0076\,s + 0.0084}{s^3 + 0.0760\,s^2 + 0.2861s + 0.0122} = \frac{0.0299}{s + 0.0442} + \frac{0.0701s + 0.0041}{(s + 0.0159)^2 + 0.5239^2}$$

Taking the inverse Laplace transform (L^{-1}) to this rational function, one gets the solution:

$$\theta_{Pade}^{[3/3]}(t) = 0.0299\exp(-0.0442t) + (0.0701\cos 0.5239t + 0.0078\sin 0.5239t)\exp(-0.0159t) \qquad (14)$$

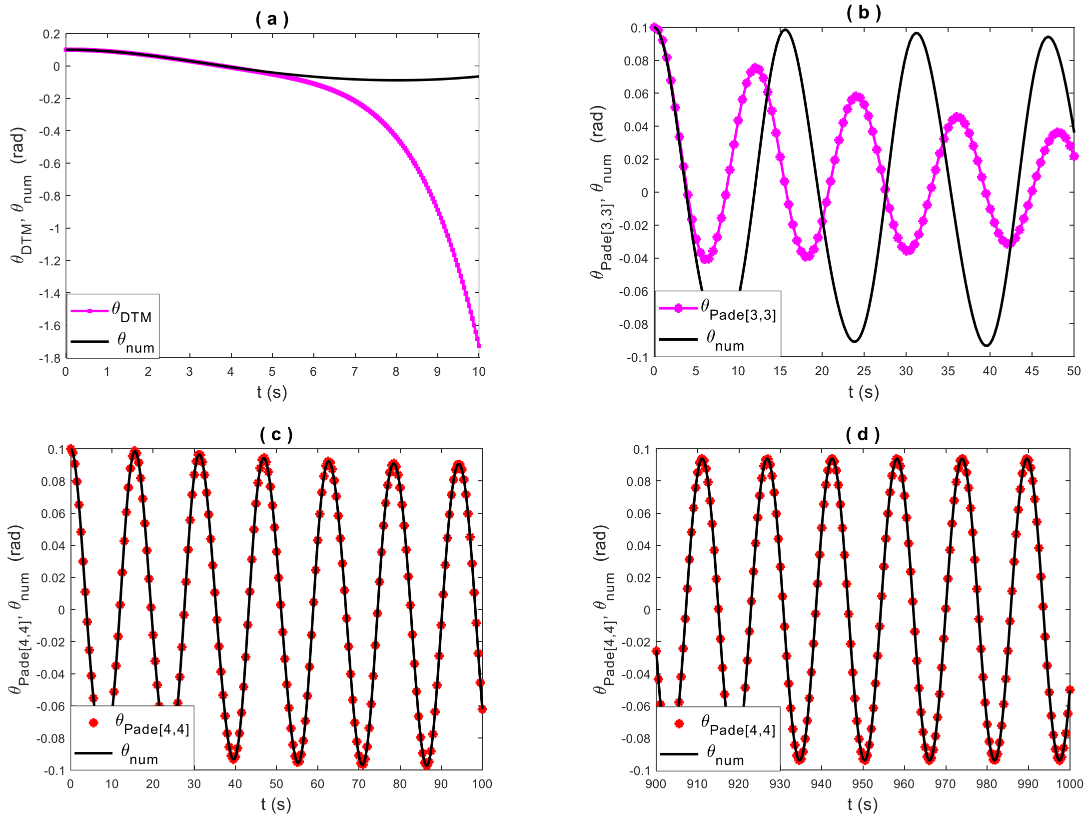

Fig. 2: Ode45 solver solution versus DTM solution (a); DTM solution with Pade [3/3] (b); DTM solution with Pade [4/4] (c, d) for $\omega = 0.4, m = 0.05, \theta(0) = 0.1, \dot{\theta}(0) = 0$

Figure 2*b* shows that this solution manages to reveal the oscillatory character of the motion but underestimates its amplitude. Let's note, however, that Pade [3/3] uses only a part of the truncated series (13). On the other hand, Pade [4/4] takes use of all the information given by (13) and its expression is:

$$\left[\frac{4}{4}\right] = \frac{0.1s^3 + 0.0013\,s^2 + 0.0660\,s + 0.0002}{s^4 + 0.0127\,s^3 + 0.8520\,s^2 + 0.0020\,s + 0.1107} = \frac{0.094\,s + 0.0003}{s^2 + 0.16} + \frac{0.006s - 0.0002}{(s + 0.0063)^2 + 0.8318^2}$$

Applying again the transform L^{-1}, one finds:

$$\theta_{Pade}^{[4/4]}(t) = 0.094\cos 0.4t + 0.0075\sin 0.4t + (0.006\cos 0.8318t - 0.00029\sin 0.8318t)\exp(-0.0063t) \quad (15)$$

Figures 2 *c*, *d* proves that the function (15) is in outstanding consensus with the numerical solution both for transitory and stationary stages of the motion.

Subcase 1.2: $\omega = 0.9, m = 0.1, \theta(0) = 0.1, \dot{\theta}(0) = 0$

We chosed this pair (ω, m) to demonstrate that the improvement brought by the Pade approximants to the DTM solution produce the same beneficial effects not only in the case of the small-amplitude oscillations described previously, but also for large amplitudes and complicated transient behaviors.

Figure 3, which contains the same type of information as Figure 2, shows that Pade [4/4] allows obtaining high-quality approximate analytical solutions for linear roll equation. The three laws are:

$$\theta_{DTM}(t) = 0.1 + 0.0154\,t^2 - 0.6498\cdot 10^{-4}t^3 - 0.0043\,t^4 + 0.1304\cdot 10^{-4}t^5 + 0.1894\cdot 10^{-3}t^6 - \\ - 0.5574\cdot 10^{-6}t^7 - 0.3658\cdot 10^{-5}t^8$$

$$\theta_{Pade}^{[3/3]}(t) = 0.1093\exp(-0.0009t) + (-0.0093\cos 1.8226t + 0.00011\sin 1.8226t)\exp(-0.0013t) \quad (16)$$

$$\theta_{Pade}^{[4/4]}(t) = -0.839\cos 0.9t + 0.081\sin 0.9t + (0.939\cos 0.8318t - 0.0735\sin 0.8318t)\exp(-0.0063t)$$

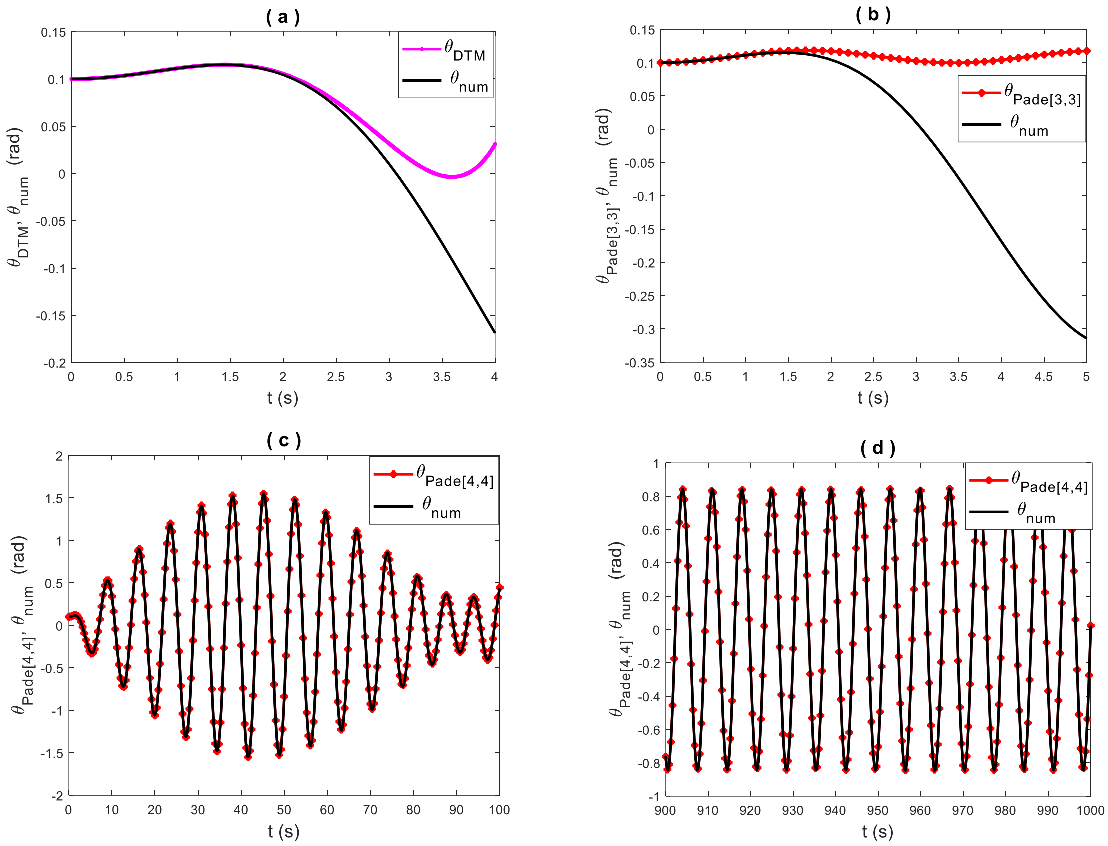

Fig. 3: The same type of results as in Fig. 2 but for $\omega = 0.9, m = 0.1$.

Case II: $m = 0$

Equation (7) becomes:

$$\ddot{\theta} + d_1\dot{\theta} + d_3\dot{\theta}^3 + k_1\theta + k_3\theta^3 = 0, \theta(0) = \theta_0, \dot{\theta}(0) = \dot{\theta}_0 \quad (17)$$

and has no exact analytical solution. The oscillations described by (17) are damped with a rate of decay depending on the coefficients d_1 and d_3. Regardless the wave frequency ω, for the initial conditions $\theta(0) = 0.1, \dot{\theta}(0) = 0$, we have that:

$$\theta_{DTM}(t) = 0.1 - 0.0343\,t^2 + 0.1449\cdot 10^{-3}t^3 + 0.0019\,t^4 - 0.1771\cdot 10^{-5}t^5 - 0.3729\cdot 10^{-4}t^6 -$$

$$-0.1232\cdot10^{-5}t^{7}-0.308\cdot10^{-6}t^{8} \tag{18}$$

and

$$\theta_{Pade}^{[3/3]}(t)=-0.0001\exp(-1.3053t)+(0.1001\cos0.8268t+0.00019\sin0.8268t)\exp(-0.0034t) \tag{19}$$

$$\theta_{Pade}^{[4/4]}(t)\cong(0.1\cos0.8294t+0.000892\sin0.8294t)\exp(-0.0076t) \tag{20}$$

Figure 4*a* highlights the small radius of convergence of the truncated series (18). The solution (19) follows the numerical one extremely well from the frequency point of view but overestimates the amplitude so that the vanishing of the initial disturbance $\theta(0)$ will occur in a longer time (see Figure 4*b*). Finally, a comparison on numerical results with $\theta_{Pade}^{[4/4]}(t)$ indicates the excellent accuracy of the solution (20) (see Figure 4*c*).

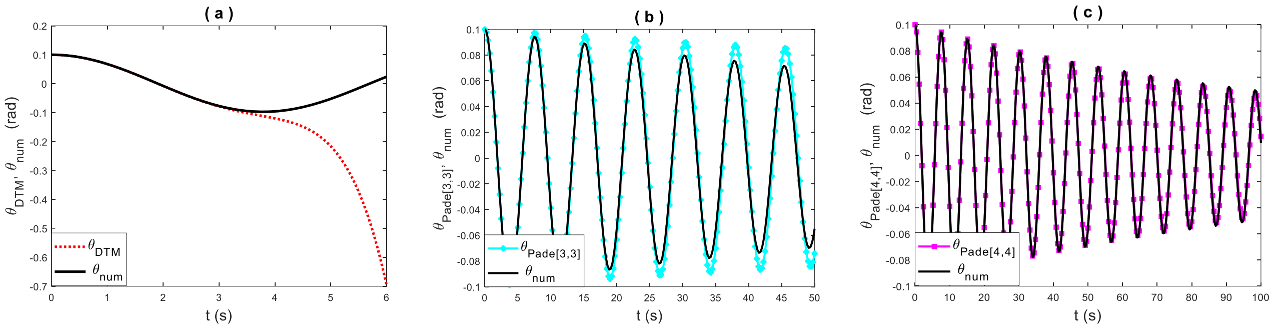

Fig. 4: Comparison between numerical solution of (17) and (a) DTM solution (18), (b) $\theta_{Pade}^{[3/3]}$ solution (19), respectively, (c) $\theta_{Pade}^{[4/4]}$ solution (20)

Case II: $m \neq 0$

This time, the solution obtained using Pade [4/4] is, for most combinations (ω, m), far from the numerical one. To understand the reason, let us follow Figure 5, which shows the position in the complex plane of the roots of the polynomial Q_4 for $\omega = 0.9$, $m \in [0, 0.15]$ and various initial seeds. To achieve a bordered periodic solution at least two roots must be pure imaginary. The remaining roots may eventually have real, but negative, parts. For example, in the linear case, for $\omega = 0.9$ the roots are $r_{1,2} = \pm 0.9i$, $r_{3,4} = -0.0063 \pm 0.8318i$ regardless of amplitude *m*.

Figure 5 shows that the four roots are, two by two, complex conjugates but, for overwhelming majority of *m* values, the real parts are negative (the initial excitation is estinguishing in time) or positive (the solution tends to infinity). The initial conditions significantly affect the location of the roots in the complex plane and there is a risk that all roots have non-zero real parts (see Figure 5*c*).

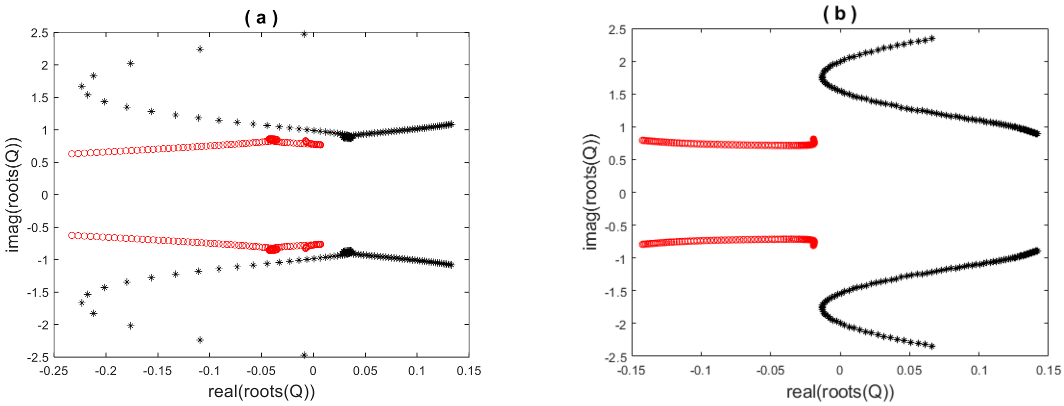

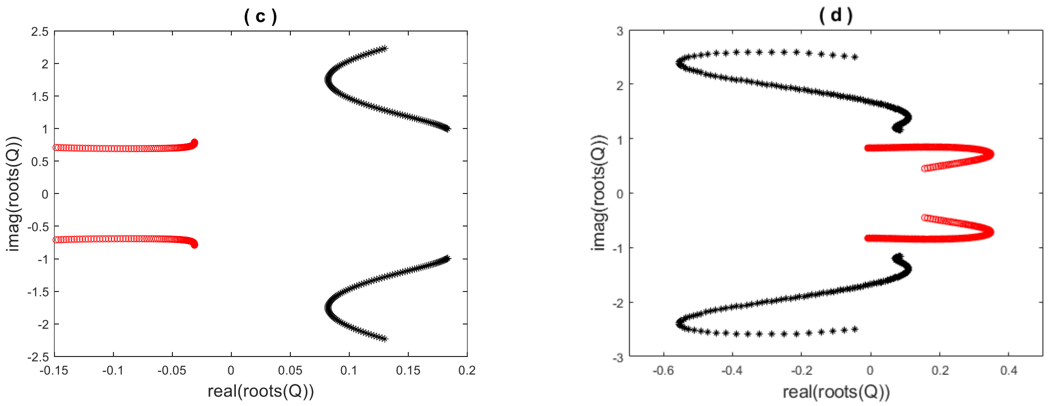

Fig. 5: The location of the roots of polynomial Q in the complex plane for $\omega = 0.9$, $m \in [0, 0.15]$ and the initial conditions:

(a) $\theta(0) = 0.1, \dot{\theta}(0) = 0$; (b) $\theta(0) = 0.3, \dot{\theta}(0) = 0$; (c) $\theta(0) = 0.4, \dot{\theta}(0) = 0$; (d) $\theta(0) = 0.0, \dot{\theta}(0) = 0.1$

In figure 5*d*, zero real parts are obtained for m = 0.03566 and m = 0.00171. More precisely, for the two values of amplitude m, the roots are $\pm 1.6769i$, $0.1652 \pm 0.8458i$ and $\pm 0.8284i$, $-0.1573 \pm 2.5643i$. In the first instance, the solution $\theta_{Pade}^{[4/4]}$ is boundless (see Figure 6*a*) while for m = 0.00171 the roll oscillation amplitude is overestimated (see Figure 6*b*).

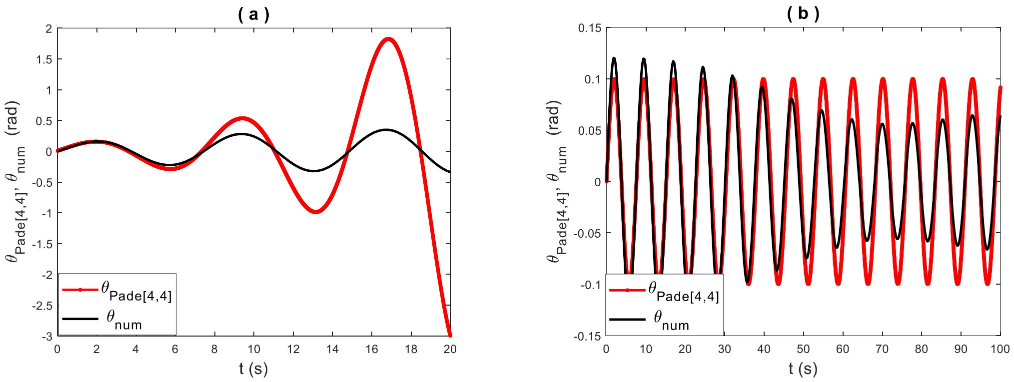

Fig. 6: Comparison between numerical solution of (7) and $\theta_{Pade}^{[4/4]}$ solution for $\omega = 0.9$, $\theta(0) = 0.0, \dot{\theta}(0) = 0.1$ and (a) m = 0.03566; (b) m = 0.00171.

To the question "How could we still use DTM and its improvements in solving equation (7) there could be more attempts. We present below two of them.

Attempt 1:
A natural continuation of the previous study involves the use of higher-order Pade approximants. Considering $k = 6,7,8,9$ in the recursive scheme (8), one finds:

$$k=6: 56\theta(8)+7d_1\theta(7)+d_3\big(21\theta^2(1)\theta(7)+72\theta(1)\theta(2)\theta(6)+90\theta(1)\theta(3)\theta(5)+48\theta(1)\theta^2(4)+ +144\theta(2)\theta(3)\theta(4)+60\theta^2(2)\theta(5)+27\theta^3(3)\big)+k_1\theta(6)+k_3\big(3\theta^2(0)\theta(6)+6\theta(0)\theta(1)\theta(5)+ +6\theta(0)\theta(2)\theta(4)+3\theta(0)\theta^2(3)+6\theta(1)\theta(2)\theta(3)+3\theta^2(1)\theta(4)+\theta^3(2)\big)=-m\frac{\omega^6}{720}$$

$$k=7: 72\theta(9)+8d_1\theta(8)+d_3\big(24\theta^2(1)\theta(8)+84\theta(1)\theta(2)\theta(7)+120\theta(1)\theta(4)\theta(5)+180\theta(2)\theta(3)\theta(5)+ +108\theta(1)\theta(3)\theta(6)+72\theta^2(2)\theta(6)+96\theta(2)\theta^2(4)+108\theta^2(3)\theta(4)\big)+k_1\theta(7)+k_3\big(3\theta^2(0)\theta(7)+ +6\theta(0)\theta(1)\theta(6)+6\theta(0)\theta(3)\theta(4)+6\theta(1)\theta(2)\theta(4)+3\theta^2(1)\theta(5)+3\theta(1)\theta^2(3)+3\theta^2(2)\theta(3)\big)=0$$

$$k=8: 90\theta(10)+9d_1\theta(9)+d_3\big(27\theta^2(1)\theta(9)+96\theta(1)\theta(2)\theta(8)+126\theta(1)\theta(3)\theta(7)+144\theta(1)\theta(4)\theta(6)+$$
$$+75\theta(1)\theta^2(5)+84\theta^2(2)\theta(7)+216\theta(2)\theta(3)\theta(6)+240\theta(2)\theta(4)\theta(5)+135\theta^2(3)\theta(5)+144\theta(3)\theta^2(4)\big)$$
$$+k_1\theta(8)+k_3\big(3\theta^2(0)\theta(8)+6\theta(0)\theta(1)\theta(7)+6\theta(0)\theta(2)\theta(6)+6\theta(0)\theta(3)\theta(5)+3\theta(0)\theta^2(4)+$$
$$+3\theta^2(1)\theta(6)+6\theta(1)\theta(2)\theta(5)+6\theta(1)\theta(3)\theta(4)+3\theta^2(2)\theta(4)+3\theta(2)\theta^2(3)\big)=m\frac{\omega^8}{5760}$$
$$k=9: 110\theta(11)+10d_1\theta(10)+d_3\big(30\theta^2(1)\theta(10)+108\theta(1)\theta(2)\theta(9)+144\theta(1)\theta(3)\theta(8)+168\theta(1)\theta(4)\theta(7)+$$
$$+150\theta(2)\theta^2(5)+162\theta^2(3)\theta(6)+180\theta(1)\theta(5)\theta(6)+252\theta(2)\theta(3)\theta(7)+96\theta^2(2)\theta(8)+288\theta(2)\theta(4)\theta(6)+)$$
$$+360\theta(2)\theta(3)\theta(6)+64\theta^3(4)\big)+k_1\theta(9)+k_3\big(6\theta(0)\theta(1)\theta(8)+6\theta(0)\theta(2)\theta(7)+6\theta(0)\theta(3)\theta(6)+$$
$$+6\theta(0)\theta(4)\theta(5)+3\theta^2(0)\theta(9)+3\theta^2(1)\theta(7)+6\theta(1)\theta(2)\theta(6)+6\theta(1)\theta(3)\theta(5)+6\theta(2)\theta(3)\theta(4)+$$
$$+3\theta(1)\theta^2(4)+3\theta^2(2)\theta(5)\big)=0$$

Like Pade [3/3], the Pade [5/5] approximant does not lead to sufficiently acceptable analytical solutions, so we only refer to Pade [6/6]. Figure 7, which shows the variation with *m* of the real and imaginary parts of the roots of polynomial Q, let us know that, as a rule, the six roots are settled into three complex conjugate pairs and have non-zero real parts.

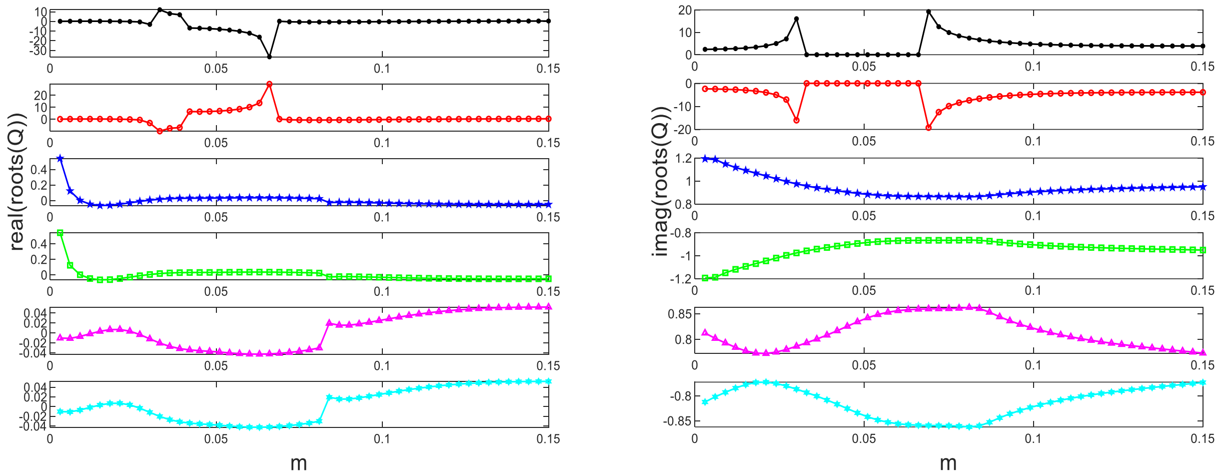

Fig. 7: The real and imaginary parts of the roots of polynomial Q
in the Pade [6/6] approximant versus the wave amplitude *m*

Consequently, the long-term solution $\theta_{Pade}^{[6/6]}$ cannot be periodic and bounded. In the short-term, i.e. for the first tens of second, there is a good correlation between θ_{num} and $\theta_{Pade}^{[6/6]}$, as shown in Figure 8.

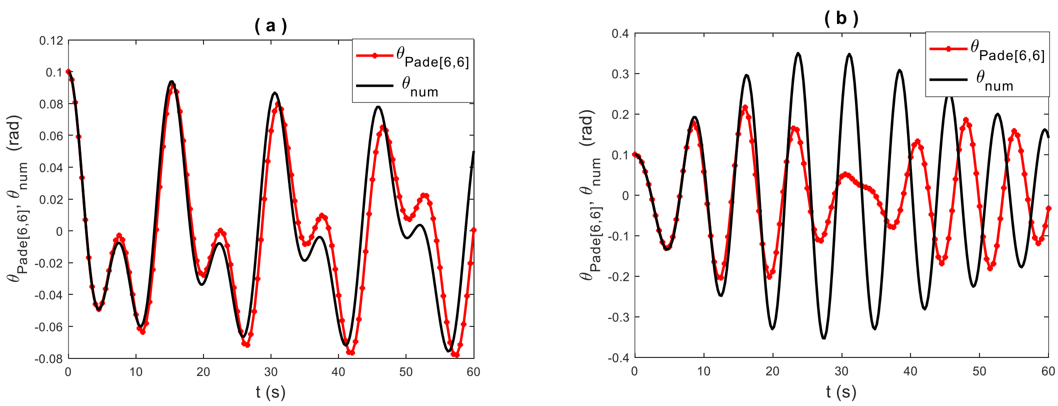

Fig. 8: Comparison between numerical solution of (7) and $\theta_{Pade}^{[6/6]}$ solution for
(a) $\omega=0.4, m=0.028$; (b) $\omega=0.9, m=0.030$

Attempt 2:

We highlighted before the fact that a severe limitation of DTM consists in the small radius of convergence. To overcome this, the time interval can be divided in small subintervals of equal length h and compute the truncated Taylor series (4) on each subinterval, $x_i(t)=\sum_{k=0}^{m}U_i(k)(t-t_i)^k, i=1,2,\ldots$, where $t_i=(i-1)h$ and the initial conditions on each subinterval $[t_i,t_{i+1}]$ are the values of x_i and its temporal derivatives in t_i [10]. In this way, the values of t are no longer far from the center t_i of the series.

Let us first gain some experience on the case of the damped oscillator analysed in case II. From numerical point of view, it will be important not only the length h of each subinterval $[t_i,t_{i+1}]$ but also the way in which the derivative $d\theta/dt(t_i)$ is calculated. We chose the classical version $\frac{d\theta}{dt}(t_i)\cong\frac{\theta(t_i)-\theta(t_i-dt)}{dt}$, where $dt=h/M$, M positive integer.

Thus, for $h\le 1$ and $dt\le 0.01$ this technique generates an almost identical copy of the numerical solution (see Figure 9*a*). If the value of *dt* is increased (that is, the derivative $d\theta/dt(t_i)$ is approximated more imprecisely), then the two curves gradually separate over time (see Figure 9*b*). Of course, a too high value for *h*, that is a large distance from the center of the series, will lead to a poor approximation of the exact solution, regardless of *dt* (see Figure 9*c*).

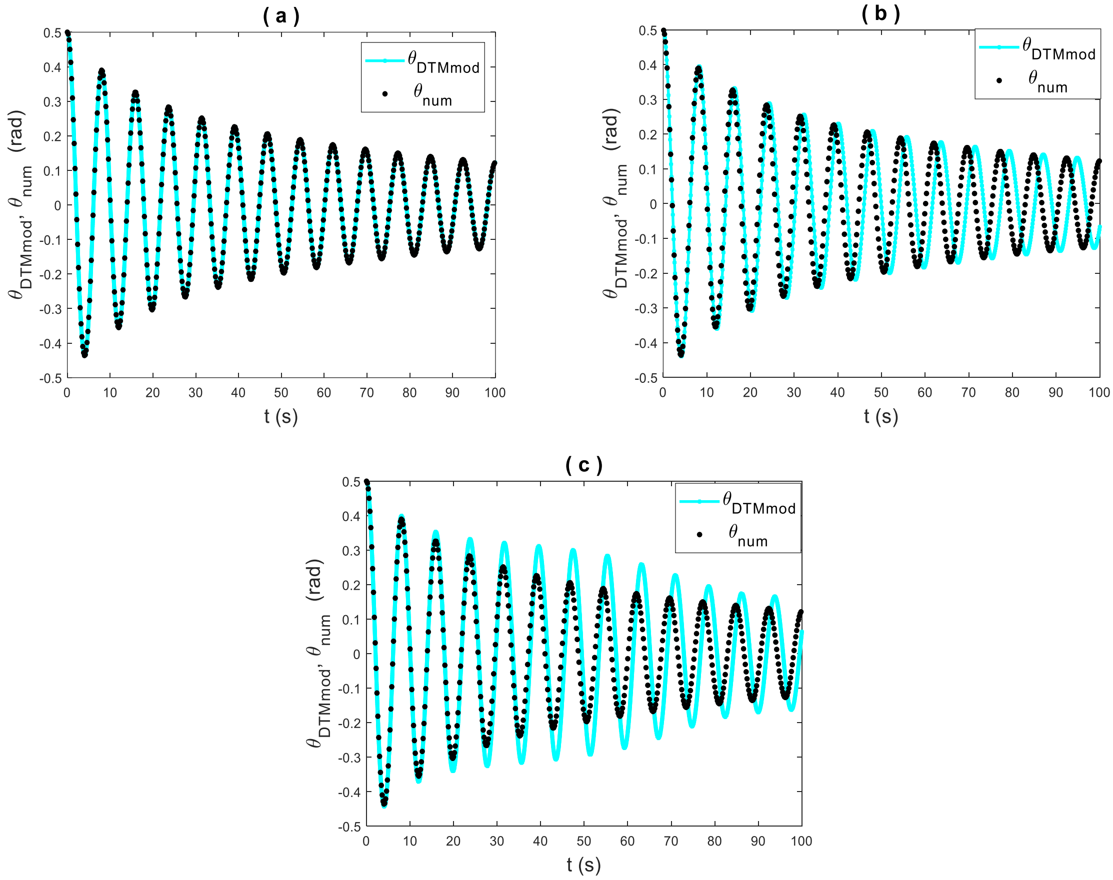

Fig. 9: Numerical solution of (17) versus Modified DTM solution for:
(a) h = 1, dt = 0.001; (b) h = 1, dt = 0.1; (c) h = 2, dt = 0.001;

Unfortunately, for the complete roll equation (7) this approach fails to generate a correct solution, no matter of the time interval splitting. It is a problem that deserves to be investigating in more detail in a future paper and that can be associated with the way in which the initial condition $d\theta/dt(t_i)$ is imposed.

4. CONCLUSIONS

In the paper, the differential transform method (DTM) and some improvements of it were employed to solve approximately a nonlinear ship roll equation. The main conclusions of the study are as follows:
a) The algorithm of the method is clear and relatively easy to implement;
b) The original DTM, which involves writing the solution in the form of a truncated Taylor series, is capable of producing reasonable results only for a small interval of time. By combining the DTM with Laplace transform and Pade approximants, an improved version of the original method is created;
c) Using Pade [4/4], we managed to practically deduce the exact solution of the linearized roll equation, which quite correctly described the roll oscillations with amplitudes below 10 – 15 degrees. The same approximant allowed us to obtain a solution with a high degree of accuracy relative to the numerical solution (produced by the *ode 45 solver* in Matlab) and for the nonlinear unforced roll equation;
d) When introducing into the nonlinear equation the wave perturbing moment, the improved DTM ceases to be effective. We gave a clear explanation for this failure and made two attempts to ameliorate it. In the first, we used the higher-order approximants Pade [5/5] and [6/6] while in the second we divided the time interval into small subintervals to bring the variable closer to the center of the Taylor series. Even some progress was found in the quality of the solution, it remained far from the numerical one both in terms of shape and amplitude.
We can therefore conclude that DTM encounters (even in its improved form) some problems in providing sufficiently good approximate analytical solutions for differential equations that contain significant nonlinearities and forcing terms.

Funding: This paper has received no external funding.
Conflicts of Interest: There is no conflict of interest.

REFERENCES

1. Al-Jawary, M.; Abd-Al-Razaq., (2016). *Analytic and numerical solution for Duffing equation*, Int.J. of Basic and Applied Sciences, 5(2), 115-119.
2. Agadjanov, E., (2006). *Numerical solution of Duffing equation by the Laplace decomposition algorithm*, Applied Mathematics and Computation, 177, 572-580.
3. Deleanu, D.; Panaitescu, M.; Panaitescu, F.V., (2020). *An accurate and fast iterative scheme for estimating the ship Rolling and capsizing in regular waves*, IOP Conf. Series: Material Science and Engineering 916 012025.
4. Deleanu, D.; Turof, M.; Dumitrache, C.L., (2022). *A trustworthy computation of the transitory and stationary responses for the ship Rolling by a modified multiple time scale method*, Int.J. of Mod. Manufact. Technol., XIV (3), 49-55.
5. He, J.H.; Jiao, M.L.; Gepreel, K.A.; Khan, Y., (2023). *Homotopy perturbation method for strongly nonlinear oscillators*, Mathematics and Computation in Simulation, 204, 243-258.
6. Aljahdaly, N.H.; Alharbi, M.A., (2022). *Semi-analytical solution of non-homogeneous Duffing oscillator equation by the Pade differential transformation algorithm*, Journal of low frequency, noise vibration and active control, 41(4), 1454-1465.
7. Zhou, J.K., (1986). *Differential transformation and its applications for electronic circuits*, Huazhong Science & Technology University Press, China, https://ph03.tci-thaijo.org/index.php/ahstr/article/view/1358.
8. El-Shahed, M., (2008). *Application of DTM to nonlinear oscillatory systems*, Communications in Nonlinear Science and Numerical Simulation, 13, 1714-1720.
9. Gokdogan, A.; Mordan, M.; Yildirim, A., (2012). *Adaptive multi-step differential transform method to solving nonlinear differential equations*, Mathematical and Computing Modeling, 55(3-4), 761-769.
10. Khatami, I.; Zahedi, E.; Zahedi, M., (2020). *Efficient solution on nonlinear Duffing equation*, J. Appl. Comput. Mech., 6(2), 219-234.
11. Faitar, C; Rusu, E., (2023). *Study on the design stage from a dimensional and energetic point of view for a marine technical wáter generator suitable for a médium size cuntainer ship*, Inventions, 8, 22-37.
12. Pedisic Buca, M.; Senjanovic, I., (2006). *Nonlinear ship rolling and capsizing*, Brodogradnja, 57(4), 321-331.

Received: February 15th, 2024 / Received in the revised form: October 20th, 2024 / Accepted: December 15th, 2024 / Paper available online: December 20th, 2024 © International Journal of Manufacturing Economics and Management.